Taylor & Francis
Taylor & Francis Group

GFF

ISSN: 1103-5897 (Print) 2000-0863 (Online) Journal homepage: http://www.tandfonline.com/loi/sgff20

Erosional and depositional subglacial streamlining processes at Skálafellsjökull, Iceland: an analogue for a new bedform continuum model

Jane K. Hart, Alexander I. Clayton, Kirk Martinez & Benjamin A. Robson

To cite this article: Jane K. Hart, Alexander I. Clayton, Kirk Martinez & Benjamin A. Robson (2018): Erosional and depositional subglacial streamlining processes at Skálafellsjökull, Iceland: an analogue for a new bedform continuum model, GFF, DOI: 10.1080/11035897.2018.1477830

To link to this article: https://doi.org/10.1080/11035897.2018.1477830

Published online: 11 Jun 2018.

GFF, 2018
https://doi.org/10.1080/11035897.2018.1477830

Taylor & Francis
Taylor & Francis Group

OPEN ACCESS Check for updates

Erosional and depositional subglacial streamlining processes at Skálafellsjökull, Iceland: an analogue for a new bedform continuum model

Jane K. Hart[a], Alexander I. Clayton[a#], Kirk Martinez[b] and Benjamin A. Robson[c]

[a]Geography and Environment, University of Southampton, Southampton, UK; [b]Electronics and Computer Science, University of Southampton, Southampton, UK; [c]Department of Geography, University of Bergen, Bergen, Norway

ABSTRACT
We combine the use of the unique Glacsweb *in situ* embedded sensors, surface velocity measurements (from dGPS and remote sensing), and UAV and field photographic surveys, to understand the subglacial processes responsible for the formation of a series of subglacial bedforms composed of both till and bedrock. There is till deformation throughout the year, with spatial and temporal variations. We estimate the ice velocity associated with the formation of a range of subglacial bedforms (9.2–31 m a^{-1}) and the erosion rate on the bedrock flutes (2.13 mm a^{-1}). We show that there is simultaneous deposition and erosion (either at the base of till or directly by ice) which generates flutes, large flutes and drumlins (rather than just depositional processes required by the instability theory). The flutes form behind obstacles associated with mobile till. Where a stationary obstacle is below a threshold height (which at this site is 1.56 m), either till tails will form behind the obstacle or a large flute will develop. Where a stationary obstacle is above a threshold height, then drumlins may form. Using these results as an analogue for larger bedforms, we discuss the bedform continuum in relation to elongation ratio, height, glacier velocity and bed mobility. These bedforms form associated with an overall net erosional regime, and once bedforms are produced, they may become fixed due to the presence of stationary obstacles, and so the resultant bedforms result from the most recent, as well as legacy, processes as they evolve over time.

ARTICLE HISTORY
Received 8 December 2017
Accepted 15 May 2018

KEYWORDS
Glaciers; wireless sensors; dGPS; remote sensing; UAV photography; structure from motion (SfM); subglacial bedforms; flutes; subglacial processes; till; drumlins

Introduction

The formation of subglacial bedforms is a fundamental process of the subglacial environment (Menzies 1979; Boulton 1987; Hart 1997; Stokes et al. 2011). Over the last 150 years many researchers have studied their form, sedimentology and distribution, and there are numerous theories for bedform formation (see recent reviews in Clark 2010; Stokes 2017). There is a general assumption that there is a continuum of subglacial elongate bedforms, formed by similar processes, but at different scales, ranging from flutes, through drumlins, megascale glacial lineations (MSGL) to streamlined hills (Rose 1987).

Investigations of the subglacial environment are logistically difficult, but recent technological developments have allowed data collection from this zone. This includes using geophysics to detect and measure the growth of drumlins (Smith & Murray 2009) and MSGLs (King et al. 2009) beneath the Antarctic ice sheet. Other developments in recent years include the studies of drumlins emerging from the glacier margin. This includes examples from Vestari-Hagafellsjökull (Hart 1995a) and Mulajökull (Johnson et al. 2010; Jónsson et al. 2014; Benediktsson et al. 2016; McCracken et al. 2016; Iverson et al. 2017 and others in this special volume).

Improvements in the resolution of remotely sensed images (as well as the use of UAV photography), combined with GIS, have allowed more detailed bedform mapping over larger areas, and enabled the quantification of bedform morphology (Greenwood & Clark 2008; Clark et al. 2009; Hughes et al. 2010; Ely et al. 2016). This includes the unexpected result that the most common shape of a drumlin is symmetrical rather than the assumed asymmetric (with a steeper stoss-side) form (Spagnolo et al. 2012). In addition it has been shown that the frequency distribution of subglacial bedforms is log-normal (Fowler et al. 2013; Hillier et al. 2013; Dowling et al. 2015; Benediktsson et al. 2016; Hillier et al., this volume), this implies that there are stochastic processes at work in the formational environment that may have an impact on frequency or location.

At the same time, mathematical models have been developed to help understand subglacial landform genesis, including the instability models of Hindmarsh (1998a, 1998b, 1999), Fowler (2000, 2009), Schoof (2002, 2007), Barchyn et al. (2016) and Iverson et al. (2017).

Over the last 40 years it has also been shown that subglacial deformation is common. Detailed geophysical and *in situ* studies have shown that 20–85% of glacier motion occurs within the subglacial sediment layer (till) rather than the ice (Boulton et al. 2001), and deformation in this layer can be modelled as a

CONTACT Jane K. Hart jhart@soton.ac.uk
#Current address: Winchester College, College St, Winchester SO23 9NA, UK.

Published online 11 Jun 2018

shear zone (Hart & Boulton 1991; van der Meer 1993; van der Wateren et al. 2000; Hooyer & Iverson 2000; Hiemstra & Rijsdijk 2003). Pore-water pressure is an important factor in determining subglacial processes and the resultant sedimentation (Boulton & Jones 1979; Alley et al. 1986; Clarke 1987; Brown et al. 1987; Hart & Boulton 1991; Hicock & Dreimanis 1992; Iverson 2010). Subglacial bedforms are a key part of the subglacial deforming layer (Boulton 1987; Hart 1997, Stokes 2017).

An essential part of understanding subglacial bedform formation is knowledge about the relationship between the internal sedimentology and the external form of the landform (see reviews in Menzies 1979; Paterson and Hooke 1995; Hart 1997; Stokes et al. 2011, 2013a). A subglacial bedform is defined as "depositional" if there is a clear relationship between the internal sedimentology/geology and its' external shape. Such bedforms often comprise a rock core surrounded by till (Crosby 1934; Boyce & Eyles 1991; Dowling et al. 2015, 2016). A bedform is defined as "erosional" if the internal sedimentology has no relationship to the external form. Unfortunately, in most bedforms the interior is not exposed.

Hart (1997) in a study of 31 drumlins from 22 sites, showed that only 6% of drumlins were depositional, 31% showed some internal deformation, but the vast majority were defined as erosional. These comprised an internal sediment unrelated to the drumlin forming event, surrounded by a thin till carapace which was related to the drumlin forming event. Examples of this from Iceland include those from Fláajökull (Jónsson et al. 2016) with a glaciofluvial core, and Solheimajökull (Schomacker et al. 2012) with a core of stiff till, both surrounded by a deformation till carapace. However, Hart (1997) argued that all drumlins are related to net subglacial deforming bed erosion (when more sediment is removed from a given subglacial section). The sediment flux idea associated with drumlins was also discussed by Stokes et al. (2011) in relation to the instability models discussed above (Hindmarsh 1998a, 1998b; Fowler 2009; Schoof 2002) as well by Menzies et al. (2016) associated with deformation. Hart (1997) argues that the net removal of sediment (negative flux) is associated with an increase in ice velocity or decrease in sediment supply. This concept concurs with recent measurements of high erosion rates beneath Antarctic ice streams (Smith et al. 2007, 2012). Eyles et al. (2016) proposed a similar model (erodent layer hypothesis ELH) where the drumlins form from erosion at the base of the deforming layer (subglacial deforming bed erosion – Gjessing 1965; Cuffey & Alley 1996; Hart 2006a) with the carapace formed associated with constructional deformation (Hart et al. 1990) as the glacier retreats. It has also been suggested that although the drumlins at Mulajökull were formed by deposition and erosion, the final erosional event results in the drumlins migrating down-glacier with time (Benediktsson et al. 2016; McCracken et al. 2016; and Jónsson et al. 2014; Iverson et al. 2017).

In this study, we investigate the streamlined bedforms from Skálafellsjökull, Iceland. These are composed of both till and bedrock, implying a combination of both deposition and erosion. We discuss *in situ* data from embedded wireless probes within the ice and till to investigate the type of subglacial processes occurring at the site. We compare these findings with measurements of surface velocity, combined with high resolution mapping of the foreland. We use the results from this study to investigate the specific bedforms at Skálafellsjökull, but also use these as an analogue for larger features associated with ice sheets, as part of a discussion of the conceptual bedform continuum model.

Field site and methods

The study was undertaken at Skálafellsjökull, Iceland (Fig. 1), an outlet glacier of the Vatnajökull icecap which rests on Upper Tertiary grey basalts. The area of the glacier is approximately 100 km^2 with a length of 25 km (Sigurðsson 1998). Historical records show that Skálafellsjökull was advancing during the late sixteenth and seventeenth centuries (Þorkelsson 1918–1920) and climate reconstructions for this period show relatively stable low temperatures between approximately 1550 and 1800 (Moberg et al. 2005; Vinther et al. 2009; Hannesdóttir et al. 2015). Skálafellsjökull and its northern neighbour Heinabergsjökull advanced sufficiently to coalesce in approximately 1750, and Skálafellsjökull reached its Little Ice Age Maximum extent in 1887. The two glaciers subsequently retreated until separation occurred sometime between 1929 and 1945, (Guđnason 1957; Ólafsson and Pálsson 1981; Hannesdóttir et al. 2015; Chandler et al. 2016a). Between 1945 and 1978/1982 (depending on the local position) Skálafellsjökull retreated, then advanced until 2000, and has subsequently undergone retreat (Hart, 2017).

Our study was undertaken at two locations: an *in situ* study of subglacial processes at Site A; and the mapping of bedforms in the glacier foreland at Site B. Details of the till sedimentology in the foreland are discussed in Hart (2017).The field survey is within the 1945 limit (Fig. 1c) and there has been no record of surging behaviour.

In situ *process studies*

Data were collected via the Glacsweb environmental sensor network (Hart and Martinez 2006; Martinez et al. 2017) which comprised sensor nodes (probes and geophones), base stations and a sensor network server in the UK (Fig. 2). The Glacsweb probes (0.16 m long) contained micro-sensors measuring water pressure, probe deformation, resistance, tilt and probe temperature (but only the water pressure and tilt results are discussed below). These data were recorded every hour, and transmitted to the base station located on the glacier surface. Probe data were sent diurnally via GPRS to a web server in the UK (Martinez et al. 2009).

The probes were deployed in the summer of 2008 and 2012 in a series of boreholes, which were drilled with a Kärcher HDS1000DE jet wash system. The probes were deployed beneath ice that was 58–80 m thick as this the optimum distance for radio transmission through ice (Martinez et al. 2004; Hart et al. 2006). In order to insert probes into the till, the presence of till was checked using a custom made CCD video camera. If till was present it was hydraulically excavated (Blake et al. 1992; Hart et al. 2006, 2009) by maintaining the jet at the bottom of the borehole for an extended period of time. The probes were then lowered into this space, enabling the till to subsequently close in around them. The measured depth of the probes within the till was not known, but is approximated at 0.1–0.2 m beneath the glacier base, estimated from video footage of the till excavation prior to deployment. Probes were also inserted into holes that did not reach the bed in order to study the ice behaviour.

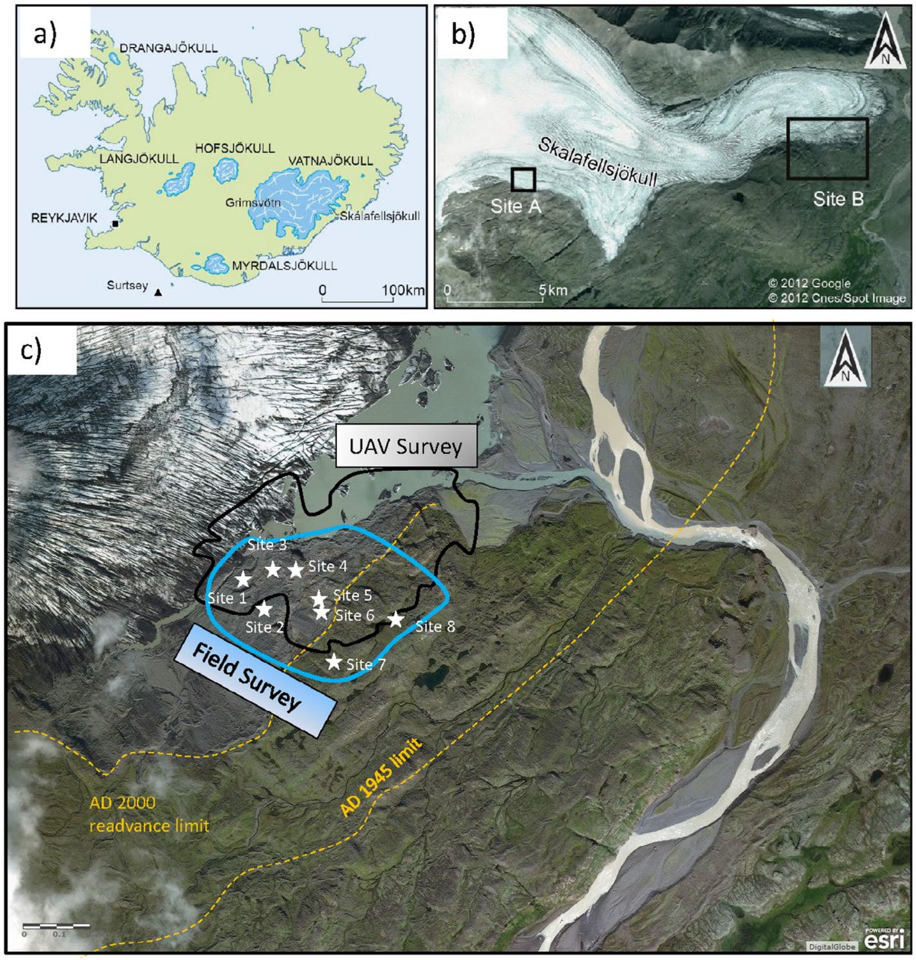

Figure 1. (a) The location of Skálafellsjökull in Iceland; (b) Detail of the glacier and location of the sites, and the location of the glacier centre line velocity profile and Little Ice Age Limit, (c) Detail of the foreland (Site B), showing the location of the UAV survey (outlined in black), field survey (outlined in blue) and detailed sites, and the AD 2000 readvance limit and AD 1945 limit.

Water pressure was measured in meters water equivalent (m W.E.) and calculated as a percentage of glacier thickness. The glacier thickness was determined from a 50 MHz Ground Penetrating Radar (GPR) survey and TOPCON GPS mounted on the base station which recorded positions throughout the year. The water depths were calibrated against the measured water depths in the borehole immediately after probe deployment.

The Glacsweb probes measure tilt with two dual axis 180° MEMS accelerometers. Values of 0° x-tilt and y-tilt represent the probe standing vertically, these were calibrated in the laboratory, and dip was calculated by trigonometry. The probe is normally almost vertical during deployment and inclines towards the horizontal as the glacier moves over the till (Hart et al. 2009).

In order to estimate glacier surface melt, we used the positive degree day algorithm (Braithwaite 1995; Hock 2003). Air temperature data were obtained from a meteorological station sited on the base station and, during short periods of mechanical failure, from a transfer function applied to data from the neighbouring Icelandic meteorological station at Höfn (approximately 30 km away to the East at sea level) (Hart et al. 2015). We used the degree day factors derived from Satujökull, Iceland (Johannesson et al. 1995), 5.6 mm d^{-1} °C^{-1} for snow and 7.7 mm d^{-1} °C^{-1} for ice. Albedo was calculated from MODIS data, using the threshold between ice and snow to be 0.45, on a 30×30 m grid ASTER DEM. This has accuracy in Arctic areas of between 5 and 10 m (Rees 2012), and although the SRTM DEM is generally more accurate it is not available for areas north of 60°N (Frey & Paul 2012).

We define the seasons based on the melt rate/air temperature. During winter there is no melt apart from positive degree days (approximate day of year (DOY) 290-102); during the rest of the year there is continuous surface melt (melt-season). During spring there is a low but constant melt (~ DOY 103-155), summer is marked by a dramatic increase in melt (~ DOY 156-252), and autumn reflects a distinctly lower level of melt, usually with temperatures going below zero at night (~ DOY 253-289) (shown on Fig. 3a).

Glacier velocity measurements

Estimates of surface velocity were made in two ways: remote sensing of the whole glacier and a series of point measurements of velocity from four GPS stations.

Surface glacier velocity was determined using the speckle tracking algorithm within the European Space Agency (ESA) Sentinel Application Platform (SNAP). Intensity tracking is less

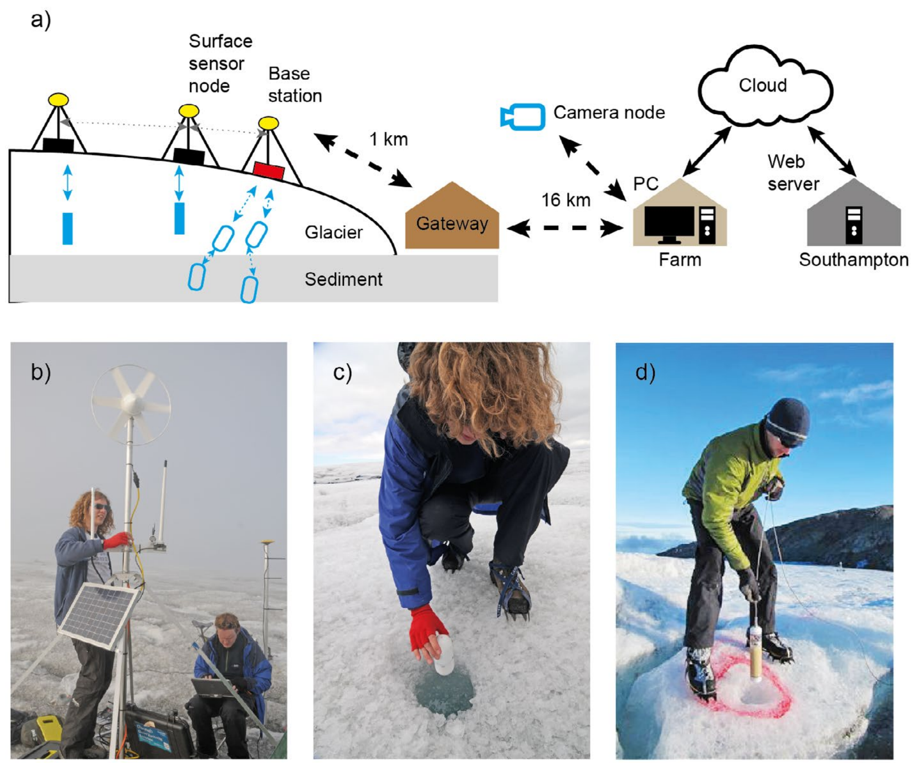

Figure 2. Glacsweb environmental sensor network: (a) schematic diagram; (b) photograph showing the base station, (c) photograph showing the insertion of a probe, (d) photograph of the installation of a custom built geophone

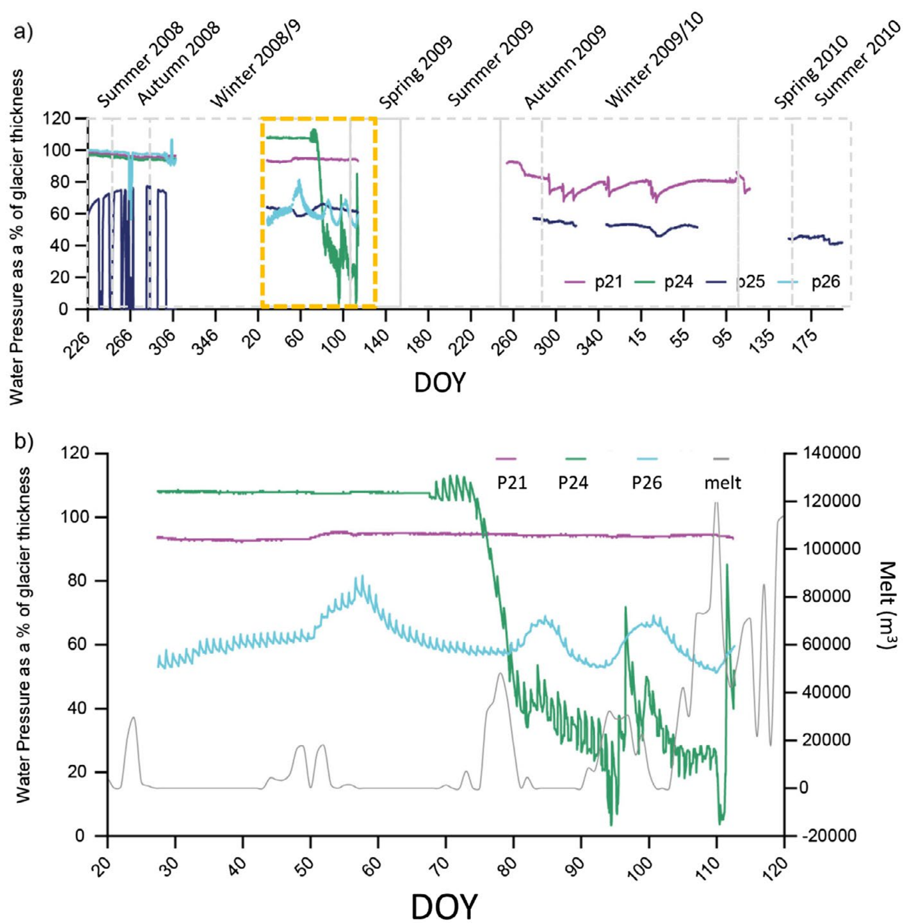

Figure 3. Probe Data: (a) *In situ* results water pressure (Till probes: P21, P24, P25; Ice probe: P26); (b) Detail from winter/spring 2009 (time shown above by dashed box).

Table 1. Attributes of the Skálafellsjökull UAV survey.

Attribute	Value
Survey altitude (m)	100
Photo endlap (%)	80
Photo sidelap (%)	60
No. of images captured	117
Image resolution (m)	0.05
DEM resolution(m)	0.04 m/pixel
Point density	605 points/km
Error	0.0022 m

precise than interferometry but given the high temporal correlation of glacier surfaces, it is much more robust (Pritchard et al., 2005). Two Single Look Complex (SLC) TerraSAR-X images with an eleven day temporal baseline (5th and 16th October 2012) were calibrated and co-registered together using a DEM-assisted co-registration. The DEM was derived from airborne LiDAR data provided at 5 metre resolution from the Icelandic National Land Survey.

Velocities were then calculated using cross-correlation with a 5×5 moving window and a search distance of 64 pixels. Any displacements that had a cross-correlation threshold of 0.01 were removed, and the displacements were averaged to a 5×5 mean grid and converted to ground range.

On the glacier, 4 dual frequency Leica dGPS stations were installed at Site A, with a local base station on the moraine (2012–2013). The stations recorded measurements at 15 s sampling rate continuously during the summer and 2 h a day during the winter. The GPS data were processed using TRACK (v. 1.24), the kinematic software package developed by Massachusetts Institute of Technology (MIT) (http://www.unavco.org/, http://geoweb.mit.edu/~tah/track_example/). This enabled us to reconstruct both daily and annual velocities.

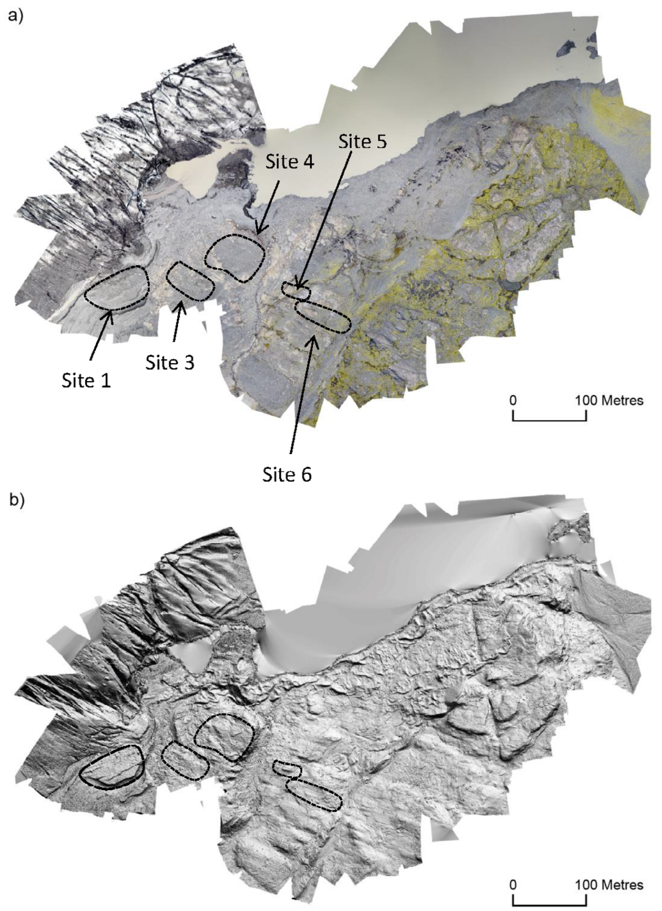

Figure 4. (a) Orthophotograph of the area mapped with the UAV (with sites shown); (b) Hill – shaded DEM of the survey area. Hill shade is from 20° to a 45° azimuth with a *z*-factor scaling of 2 (with sites shown).

Survey

The foreland was investigated at two scales (Fig. 1c). Firstly by a large scale UAV photographic survey in 2013, and then a field survey in 2015 (of approximately the same area), where specific bedforms were identified and 8 sites examined in detail (including photogrammetric surveys).

For the large scale UAV photographic survey, a Quest 200 fixed wing UAV carrying a Panasonic DMC- LX5 camera was used. Fifteen ground control points (2 m^2 targets) were employed which were surveyed using a Leica RTK dGPS deployed in Real-time Kinematic (RTK) mode. The UAV was used in conjunction with a Leica dGPS. The survey was part of a larger survey of the Skálafellsjökull foreland (see details in Hackney & Clayton 2015) that was used to produce a large scale geomorphic map (Chandler et al. 2016b).

The data were processed using the Structure from Motion (SfM) technique (Snavely et al. 2008; Westoby et al. 2012; Hackney & Clayton 2015; Ely et al. 2017) using AgiSoft PhotoScan software. The details are shown in Table 1. The resulting orthophoto had a spatial resolution of 0.05 m and the DEM 0.1 m (Fig. 4a). These were then imported into ArcMap where it was hillshaded orthogonally to ice flow (20°, 200°) in order to illuminate lineations. A *z*-factor exaggeration of 2 was also applied to aid identification of the landforms. A contrasting hill shade of 290° was used to check for unusual forms and identify the initiation point of lineations (Fig. 4b). The flute length and spacing were then measured. The flute spacing was established by mapping the crestlines of each identifiable feature and determined as crest to crest distance (Hoppe & Schytt 1953).

A field survey was undertaken (Fig. 1c) to ground truth the aerial survey and examine individual streamlined bedforms in detail. During the field survey the different types of bedforms were examined, and photographic surveys were taken in specific areas of the fluted till areas. The field survey allowed the percentage of till in each of the bedforms to be determined. The bedforms were imaged with a Nikon D610 digital camera using both still and video photography. The close range digital photography was used to reconstruct 3D structure using the Structure from Motion (SfM) technique in AgiSoft PhotoScan (Fig. 5). Table 2 shows the details of the imaging. The orthophotos were then used to measure the bedform parameters; width, height, spacing, lengths, as well as calculate elongation ratio (length/width). For some of the flutes, the lengths were difficult to ascertain because the fluted area had been eroded by post depositional processes. In those cases the maximum exposed length was measured. The resultant elongation ratio would be an underestimation.

We also used the historical glacier records (discussed above) combined with the survey data to estimate an erosion rate over the bedrock flutes. This was calculated by the height of the

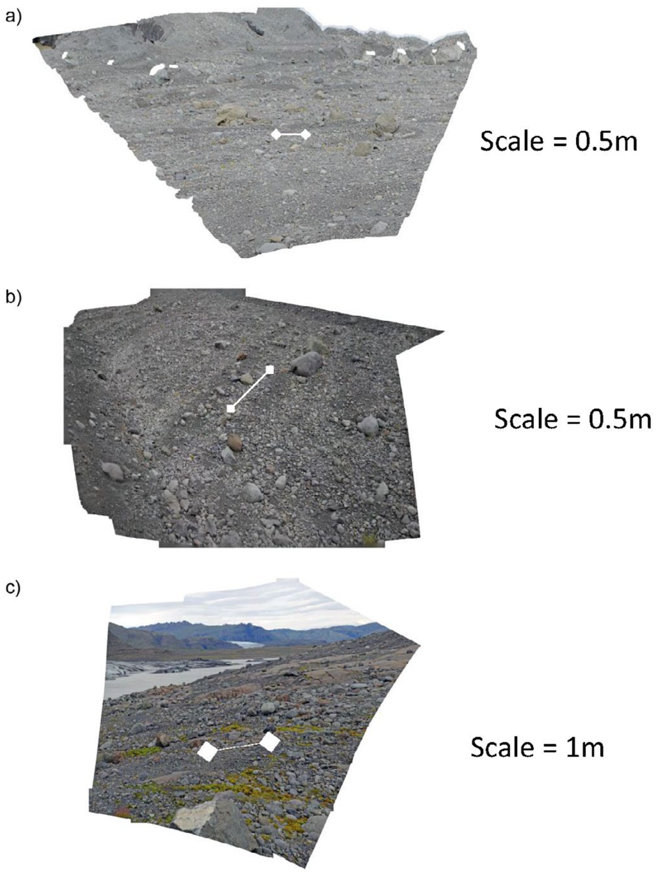

Figure 5. Orthophotographs of the flute areas: (a) Site 1a (image looking towards the north east); (b) Site 1b (image looking towards the south east); (c) Site 4 (image looking towards the north east) (the scale is marked by the scale bar in the approximate centre of the image).

Table 2. Details of the Photogrammetric survey.

Site	Aligned photographs	Tie points	Error
1a	46	9098	2.96 mm
1a (video)	501	1269	1.95 mm
1b	7	5614	0.859 mm
1b (video)	273	1269	1.95 mm
1c	6	2149	0.427 mm
3	4	943	0.629 cm

bedform divided by the minimum length of time the glacier was present at each site. The date of retreat was estimated from the air photography and satellite data discussed in Hart (2017) and the date of advance from a linear extrapolation of the historical records. Given the relatively stable low temperatures during 1550–1800, a linear relationship would provide a realistic estimate of the rate of glacier advance 1600–1750.

Results and interpretation

In situ *process studies*

The data collection was successful with data collected 2008–2010 and 2012–2013 (discussed in detail in Hart et al. 2015). Fig. 3a shows the water pressure recorded from three *in situ* probes from 2008 to 2010, three are in the till (P21, P24, P25), and one in the ice (P26). In general, water pressure was high throughout the year, with some distinct events during the winter/spring of 2009 and short-term events during winter 2009/2010. The probes were deployed in an area approximately 30×10 m.

Table 3. Melt season tilt variation.

	Glacier thickness	Distance from site closest to centreline (P31)	Mean season tilt variation (s.d. as a % of mean tilt)
P21	58	40 m	90%
P25	59.5	25 m	−76%
P31	69	–	−21%
P32	67.5	10 m	8%

Tilt data from the till probes shows that there was movement all year, although the winter rate is 60% of the melt-season rate. However, superimposed on this general trend is significant local variation. Table 3 shows how the tilt varies (expressed as the standard deviation as a percentage of the mean melt season tilt) over the relatively small area studied (measured from the probe closest to the centreline P31) during the melt-season. This indicates the variation in the amount of deformation beneath the deforming layer on a relatively small scale, reflecting changes in pore water pressure or the relationship to obstacles.

Figure 3b shows detail of winter/spring 2009. Probe 21 (in the till) has a constant high water pressure. Probe 26 (in the ice) has a diurnal cycle and responds to high melt water inputs (with a five day lag). In contrast, Probe 24 (in the till) has a very different pattern, which is not recorded by any other of the probes. At the start of the record (DOY 23-66), Probe 24 behaves in a similar way to Probe 21, with constant high water pressure and no relationship to any high melt water events. However, the water pressure values are much higher, over 100%. At 15:00 on DOY 67 the water pressure changes slightly and by the following day a diurnal cycle had begun. This comprised water pressures rising abruptly at noon (to even higher levels) and then slowly declining over the subsequent twenty-four hours. This pattern continued until DOY 72, after which time the water pressure significantly declined and responded to surface melt. There was still a diurnal cycle, but now it was less regular and comprised a rapid rise at 12:00, slight decline during the afternoon and then a sharp fall around 23:00.

We know that initially Probe 24 was located within the till where it was not affected by short-term changes in surface melt water. We suggest that the extreme high pressures were not related to melt water forcing events (as proposed by Murray & Clarke 1995) but instead relate to a local physical constraint, for example, an obstacle within the deforming layer such as a larger clast or stiffer till. On DOY 67 a change happened to the probe, as it began to experience a high water pressure diurnal cycle. This must imply that it came in contact with the subglacial meltwater system. The most realistic explanation is that it moved from a till depth of approximately 0.2 m, up to the ice/till interface itself where it came into contact with a water film. Since it was still under high water pressure conditions it must still have been constrained by the physical obstacle. The vertical movement of probes in the system has been previously recorded by the authors at Briksdalsbreen, Norway, where a probe that was initially deployed in the till, was discovered on the glacier surface. We presume the Briksdalsbreen probe was moved up to the ice/till interface and then rapidly transported up to the glacier surface via a glacier fountain event (which were recorded at Briksdalsbreen) through an englacial connection (moulin/crevasse).

On DOY 72 the water pressure recorded by Probe 24 dramatically falls and this coincides with a melt water event. These events occur throughout the winter when air temperature rises above approximately 2 °C (Hart et al. 2015) and are associated with speed-up events. We were able to record this relationship in 2012/2013 as well as being reported in the literature (Iken et al. 1983; Willis 1995; Hubbard & Nienow 1997; Anderson et al. 2004; Sugiyama et al. 2010). We suggest this event dislodged either the probe or the obstacle, so that the probe was no longer constrained by a physical obstacle, but still in direct contact with subglacial meltwater and thus could continue to respond directly to meltwater events.

Survey

The results of both surveys showed that fluting was ubiquitous, covered almost the whole area and was associated with both till and bedrock. A total of 322 flutes were mapped on the till areas from the UAV survey (Fig. 6a). The flutes have a mean spacing of 1.99 m and a unimodal distribution with a strong positive skew. Plotting the log of the measurements demonstrates that they approximate a log-normal form (Fig. 6b). The Shapiro-Wilk test (typically used with samples less than 2000) was used to test if log-normal distribution was statistically significant. The W value was 0.925 and the p value was 0. This indicates that the sample was close to log-normal (where $W = 1$) but since the p value was less than 0.05 we can reject H_o (normality) and suggest the values are not statistical significantly log-normal. The flute lengths were also measured, which also showed a unimodal distribution and positive skew (Fig. 6c).

The field study allowed the more detailed examination and classification of the bedforms (Table 4):

(1) *Till flutes* (Fig. 4a and b) – We examined three specific areas within Site 1 area. In some flutes a core stone was present, however some of flutes had been eroded by post depositional processes so it was not possible to determine whether a core stone was present or not.
(2) *Bedrock large flutes* (Fig. 7a) – The bedrock has been shaped into a streamlined form, these are large features observed from the UAV survey.
(3) Mixed till and bedrock fluted areas – These typically consist of a mixture of narrow fluted bedrock emerging from a fluted till surface (Site 3) (Fig. 4c). Site 4 comprises a large roche moutonnée feature with till and bedrock flutes on the lee-side a steep jagged cliff on the stoss side (Fig. 8b).
(4) *Composite large flutes* – these comprise both till and bedrock. Site 5 comprises streamlined bedrock with a till tail (Fig. 7c). Site 7 comprises a large feature comprised of till, but with bedrock within it (but not in the typical stoss side) (Fig. 7d).
(5) Rock-cored drumlin (Fig. 7e) –The stoss side is composed of abraded bedrock and the lee side is composed of till. These landforms have been observed at other sites in Iceland, e.g., Langjökull (Hart 1995a), Eyjabakkajökull (Schomacker et al. 2014) and described as rock cored drumlins.

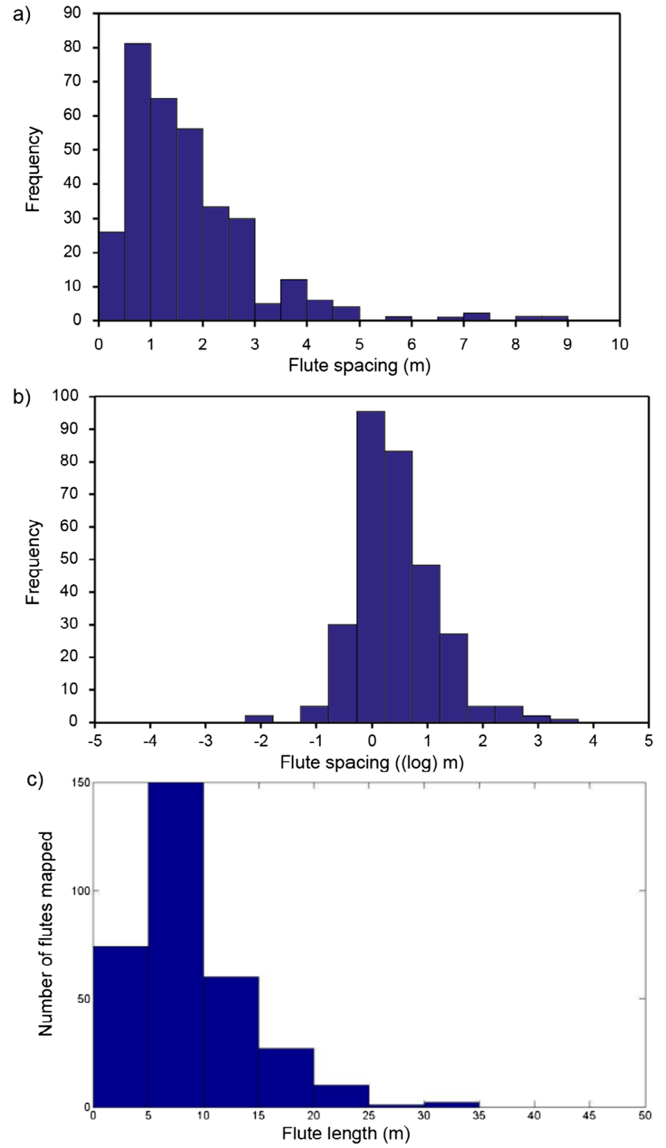

Figure 6. Results from the large scale flute survey from the till areas (n = 322: (a) histogram of flute spacing (excluding 4 outliers above 10 m); (b) Histogram of (log) flute spacing; (c) histogram of mapped flute lengths.

These features represent two distinct scales: (a) the small scale (width less than 4 m), till and bedrock flutes, and (b) the large scale (width greater than 4 m), composite and bedrock large flutes, and rock-cored drumlins. They can also be divided into features with a mobile core, such as the till flutes, and a stationary core, including bedrock and composite large flutes and rock-cored drumlins. We can quantify the relative mobility of the core by the percentage till within the bedform. We can also derive a threshold height, taken as the mid-range between the maximum flute height and minimum drumlin height (individual bedforms), which at Skálafellsjökull was 1.56 m. Table 4 also shows an estimation of the erosion rate over the bedrock flutes, which had a mean of 2.13 mm a^{-1} (s.d. 0.72).

Figure 8a shows the relationship between the elongation and the height of the feature. The till flutes are generally the same size and have a high elongation ratio, but low height. This height relates to size of the core stone. In contrast, the rock bedforms (bedrock and composite large flute, fluted rock) have an

Table 4. Details of the measured bedforms.

	Type of bedform	Number	Mean width (cm)	Mean height (cm)	Mean length (cm)	Mean spacing (crest to crest) (cm)	Elongation ratio	% till	Erosion rate (mm a^{-1})
Site 1a	Till flutes	22	25.70	16.86	>1148	34.95	>44.66	100	–
Site 1b	Till flutes	20	22.40	17.20	>1278	34.00	>57.05	100	–
Site 1c	Till flutes	10	28.96	13.32	>1310	44.20	>45.23	100	–
Site 2	Fluted bedrock	4	290.43	101.50	691.66	–	2.40	0	2.49
Site 3	Till flutes	10	20.75	19.38	1875	32.81	90.36	100	–
	Fluted bedrock	6	98.76	25.10	800	–	8	0	0.62
Site 4	Till flutes	12	24.09	25.23	3250		134.91	100	–
Site 5	Streamlined rock core/till tail	1	Rock = 300 Till = 36	Rock = 36 Till = 24	369	–	4	56	2.53
Site 6	Bedrock large flutes	4	450	64	5617	500	12.48	0	1.79
Site 7	Composite large flute	1	780	75	6686	–	8.57	98	–
Site 8	Rock cored drumlin	1	752	210	1050	–	1.40	56	–
Mean till flutes			24.02	17.84	1772.2	36.12	74.44	100	–

intermediate height and elongation ratio. The rock-cored drumlin has the greatest height and lowest elongation ratio. Figure 8b investigates the relationship between elongation ratio and obstacle mobility (percentage till). Again the till flutes cluster together.

Estimate of ice velocity during bedform formation

The remotely sensed feature tracking provided a glacier-wide estimation of surface velocity for October. This was calibrated to an annual velocity by comparing these October results with the measured annual results from the point measurements. The point measurements had a mean error estimate for North, East and height Sigma per day (m) of ±0.0045, ±0.0032, ±0.0092, respectively. We used this to construct a calibrated glacier central line velocity profile (location shown in Fig. 1b and results in Fig. 9).

Assuming the pattern of ice velocities remained similar when the glacier was more extensive, we use the distance from the margin/glacier velocity relationship shown in Fig. 9, to make an estimate of glacier velocity when the bedforms were formed. This is reasonable assumption to make as the factors that control glacier velocity such as rate of meltwater delivery, bedrock topography and bedrock geology would have remained relatively constant. Since it is not known how long the bedforms take to develop (i.e., which ice limit they relate to), we have taken the maximum as the Little Ice Age limit (Fig. 1b) (bedform location 1400–1700 m from Little Ice Age limit), and a lower measurement from the 1945 (limit of the field survey area, Fig. 1c) (bedform location 115–530 m from 1945 limit). This gives a mean velocity estimate of 31 and 18 m a^{-1}, respectively. The current till flutes formed at Site 1 may have been formed within 50 m of the 2012 limit giving a velocity of 9.2 m a^{-1}.

Discussion

The survey showed that fluting occurred everywhere in the exposed subglacial surface on the foreland, irrespective of geology. It is then not unreasonable to suggest that the probe behaviour, which recorded the subglacial processes, may be related to active flute forming conditions. The results from the *in situ* studies show that the till was deforming and that deformation occurred throughout the whole year, and there was local variability in the amount of tilt.

We described one unusual event that occurred during winter/spring 2009, where a probe (Probe 24) must have changed location, from within the till (water pressure over 100% of glacier depth) to the ice/sediment interface (high but diurnal water pressure), to another location at the ice/till interface after a surface melt-related speed-up event (diurnal and meltwater input related variability). We have proposed that initially the probe was held behind a physical obstacle. One interpretation is that the initial obstacle could have been the core stone of a flute (Fig. 10a), and then continued deformation of the till caused the probe to move up to the ice/till interface behind the clast where it came in contact with the subglacial meltwater system (Fig. 10b). At this point the probe experienced high but diurnal water pressure variations. After a winter speed-up event the probe was moved away from an obstacle (in an area with lower water pressure) but still at the ice/till interface. It is not known whether it was the probe or flute core (assuming this was the obstacle) that moved after the speed-up event. Although it is probably more likely to be the probe, since we already recorded its mobility. The probe may have been forced to flow around the flute core clast. It may have been deposited in the flute itself (Fig. 10c) (which may explain it's relatively consistent subsequent behaviour) or maybe was carried along in the interflute area.

Assuming the obstacle were a flute core stone, then it is more likely the probe moved rather than the core, since the core must be relatively stable within the deforming bed (to form the flute) and we have suggested the already interpreted probe movement. The probe may have been forced to flow around the flute core clast. It may have been deposited in the flute itself (Fig. 10c) (which may explain it's relatively consistent subsequent behaviour) or maybe was carried along in the interflute area. Given our observations about the till deformation throughout the year and local variability in tilt, combined with data about rapid winter probe (i.e., clast) movement associated with normal and speed-up conditions (irrespective of whether it was in the flute or not), we suggest that the conditions for flute formation occur all year.

Flute formation

Most researchers on flutes have supported the theories of Dyson (1952) and Boulton (1976), who suggested flutes form due to the presence of a core stone that causes the development of a small

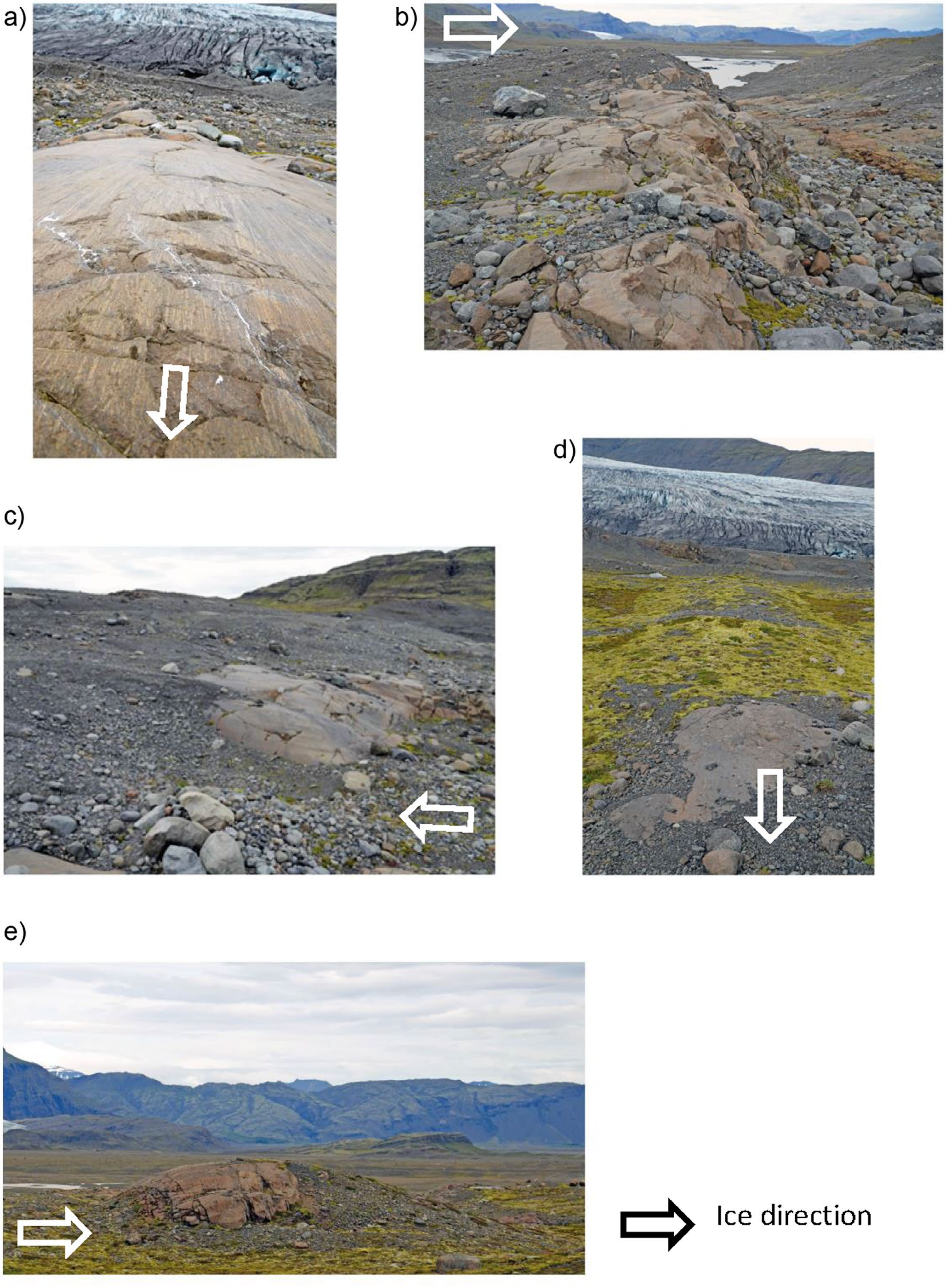

Figure 7. Photographs of the bedforms at Skálafellsjökull: (a) large fluted bedrock (Site 6) (scale 1.5 m across in foreground); (b) fluted area on the stoss side of a roche moutonnée (Site 4) (scale: view width 4 m); (c) flute with streamlined bedrock stoss side with till tail (Site 5) (scale: flute tail maximum height 0.24 m); (d) composite large flute composed of till and rock (Site 7) (scale: view width 3.5 m in foreground); (e) rock-cored drumlin (Site 8) (scale: height 2.1 m, length 7.52 m).

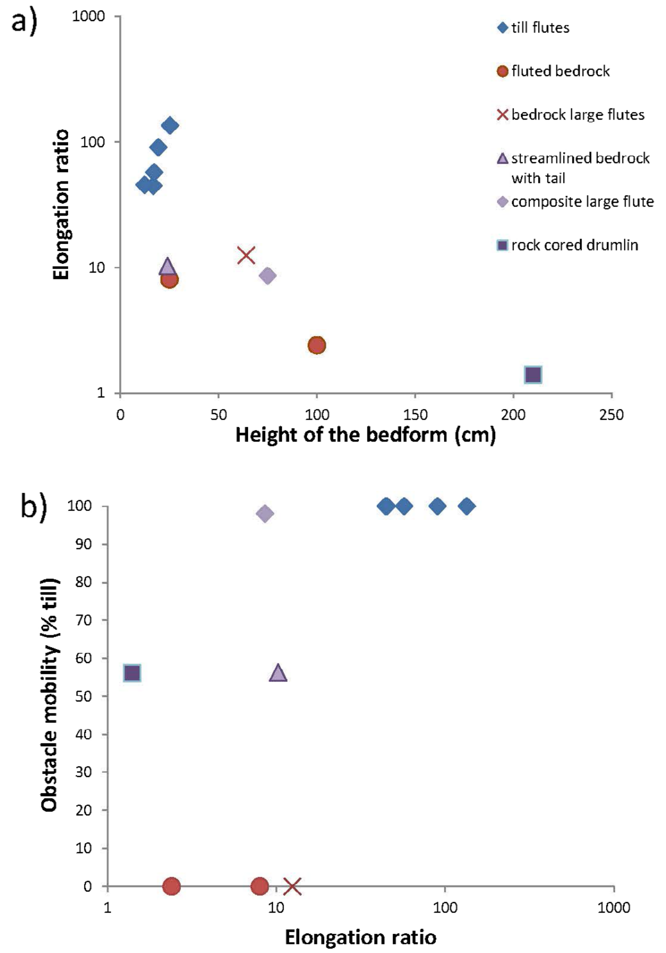

Figure 8. (a) The relationship between the mean elongation and the mean height of the feature; (b) relationship between the mean elongation ratio and the mean till mobility (% till).

lee side cavity, into which till flows, and this grows down ice (Benn 1994; Hart 2006b; Roberson et al. 2011; Eyles et al. 2015; Ely et al. 2017). Alternatively, it has been argued that flow cells exist within the till which move sediment away from the troughs to the crests, and the resultant flutes would be marked by a herring-bone pattern, often called the instability theory (Shaw and Freschauf 1973; Rose 1989; Schoof & Clarke 2008).

Table 5 shows flute characteristics from other glacier forelands as reported by the authors. Within a foreland area the flutes tend to be of a similar size. However, there are two types of forelands, as seen in the table. In some (e.g., Briksdalsbreen, Kjennsdalsbreen, Exit Glacier), flutes are the only bedform present, whilst in others (e.g., Skálafellsjökull, Vestari-Hagafellsjökull, Athabasca Glacier and Columbia Glacier) there is a clear distinction between flutes (short with high elongation ratio) and drumlins (tall with low elongation ratio) or streamlined bedrock (tall with low elongation ratio). In these environments a threshold height between the two bedforms can be calculated. This threshold height may reflect the thickness of the deforming layer or be related to the flux rate of till and/or ice associated with the lee-side cavity.

The vast majority of flutes (described in all the studies above) are composed of till, and thus these models (whether "boulder initiated" or "instability") are depositional. However at Skálafellsjökull we have evidence for both till and bedrock streamlining and that there is a relationship between scale, mobility and elongation ratio. This is evidence that there is both "deposition" and "erosion" within the deforming layer, since the till can be potentially both deposited and eroded, but the bedrock has to have been eroded into the streamlined form. The continuity of form in both till and bedrock in one flute (e.g., the composite flutes) indicates that both deposition and erosion are occurring simultaneously. Thus, we propose a new theory for bedform formation, based on this Skálafellsjökull data.

We know from numerous flute studies (as discussed above) that flute initiation cores are very common. Based on the Boulton (1976) boulder initiated deforming bed model for flutes, we suggest that the till flutes form as the till flows into a low pressure area behind the core stone (deposition). The flow of till is known because of till fabric studies (see references above), which typically show converging fabrics just proximal to the core clast (on the lee-side) and parallel with the flute (and highly oriented) further down the tail. However, we know from Skálafellsjökull that at the same time, erosion must be occurring in between the flutes. This must occur in both till and rock flutes, so within the till flutes, till must be removed from the interflute areas. This erosion will be due to either till (erosion at the base of the deforming layer, Gjessing 1965; Cuffey & Alley 1996; Hart 2006a) or directly by ice).

We were able to measure the erosion rate associated with the bedrock rock flutes, which gave a result of 2.13 mm a^{-1}. Estimates of glacial erosion for temperate glaciers are normally considered to be in the range of 1–2 mm a^{-1} (Hallet et al. 1996), but higher rates have been reported from Iceland (3–3.75 mm a^{-1}, Boulton 1982; 3.8 mm a^{-1}, Lawler et al. 1992), and our results are similar to these.

We suggest the process of simultaneous deposition behind the core stones and erosion between the flutes will remain stable within the deforming layer. This will be disrupted by the presence of either a stationary object, such as bedrock, or a mobile object larger than the threshold size (as discussed above). Where there is a relatively short stationary object, this will behave as a core stone, and till flutes will form in the lee-side (e.g., Site 5, Fig. 7c), and/or a wide composite flute will form (Site 7, Fig. 7d). Where the obstacle is larger than the threshold height a drumlin will form (Site 8, Fig. 7e). In addition, with all these examples the stationary bedrock obstacle is also undergoing erosion/streamlining.

The variety of material over which the bedforms have developed at Skálafellsjökull (till, mixed, bedrock) makes the formation of flutes by the instability theory very unlikely as this is a depositional process, rather than the simultaneous erosional and depositional process observed at this site.

Simultaneous depositional and erosion bedform model

We can apply this simultaneous deposition and erosion model to the formation of the different types of bedforms are illustrated in Fig. 11. The till flutes form associated with a mobile obstacle (core stone) (Fig. 11a). However if the till cover is thin or patchy, this may accumulate in till flutes on a bedrock surface (Fig. 11d). These were not observed at Skálafellsjökull, but have been reported in the literature (Karlén 1981). Over bedrock, flutes form behind more resistant elements of the bed (Fig. 11b), or from erosion which began from an obstacle in the till (such as

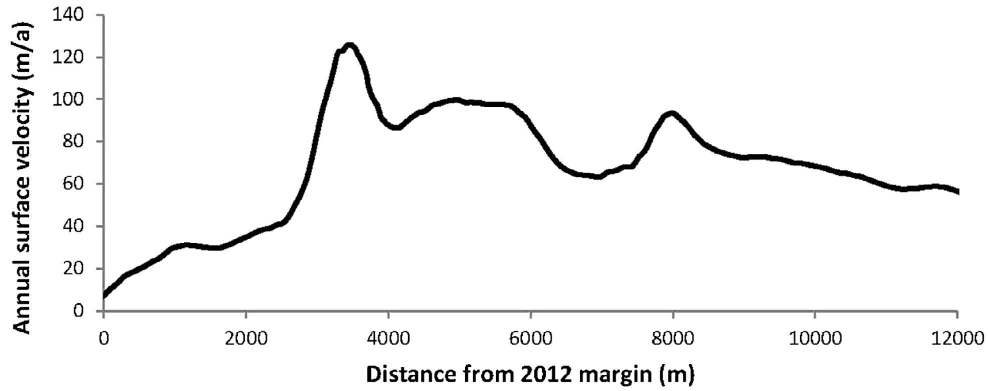

Figure 9. Annual surface velocity along the glacier centre line (based on ground truthed speckle tracked data) (location shown in Fig. 1b).

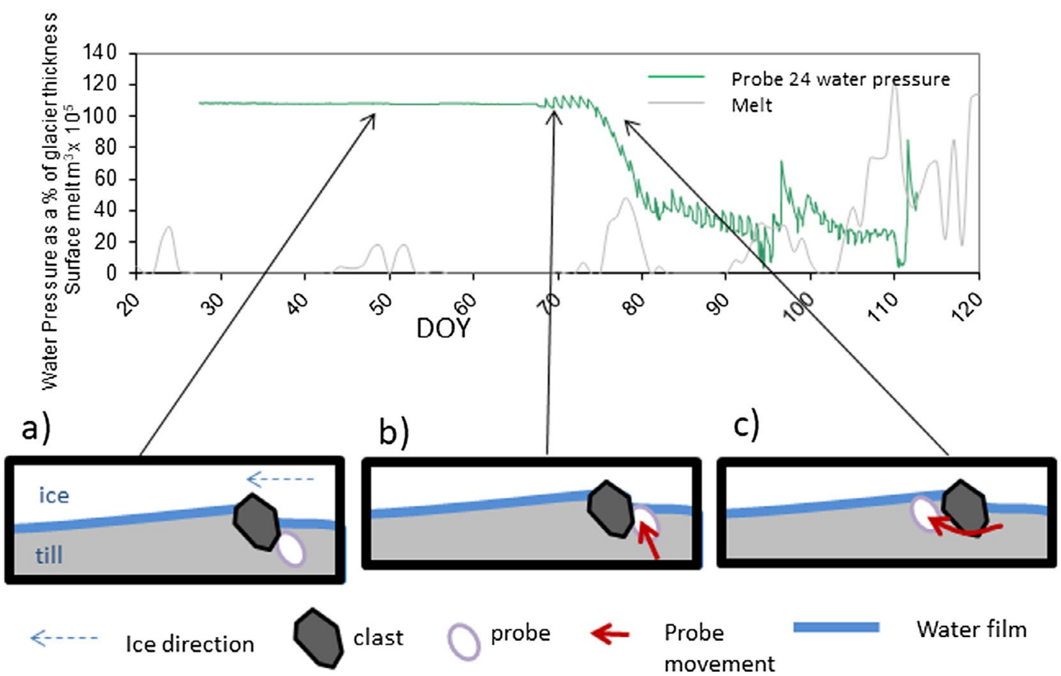

Figure 10. Schematic interpretation of the 2008 winter/spring event (upper figure: Probe 24 water pressure and melt as shown in Fig. 3b): (a) location of Probe 24 during DOY 23-66; (b) location of Probe 24 DOY 67-72; (c) location of Probe 24 DOY 73 onwards.

Table 5. Flute characteristics from some temperature glacier forelands.

	Average height (m)	Max height (m)	Threshold between flutes and other bedforms	Other streamlined bedforms
Briksdalsbreen, Norway (Hart 2006b)	0.33	0.9	–	No
Kjennsdalsbreen, Norway	0.29	0.3	–	No
Vestari-Hagafellsjokull (Hart 1995a)	0.2	0.3	0.5	Drumlins
Columbia Glacier, Alaska (Hart & Smith 1997)	0.25	0.3	0.8	Drumlins
Exit Glacier, Alaska (Hart 1995b)	0.3	0.4	–	No
Athabasca Glacier (Hart 2006a)	0.3	0.4	0.8	Streamlined bedrock
Skálafellsjökull	0.17 till 0.84 bedrock	0.28 till 1.02 bedrock	1.56	Yes

in Fig. 11d) but continued in this location once the obstacle was removed (legacy).

Where the bedrock is fixed, till flutes can form behind the obstacle in a similar way to the till flutes with a mobile core. Composite large flutes form where a broad (but relatively short) rock obstacle provides a core stone as part of an existing flute (Fig. 11c). These stationary obstacles may remain constant over time, and can be thought of as a framework structure within an otherwise mobile bed.

Once the obstacle is larger than a threshold depth, the till flows around the obstacle which causes the feature to become more circular (rather than linear). On bedrock this will produce a whaleback/rock drumlin, caused by erosion at the base of the deforming layer (as was demonstrated at Athabasca Glacier,

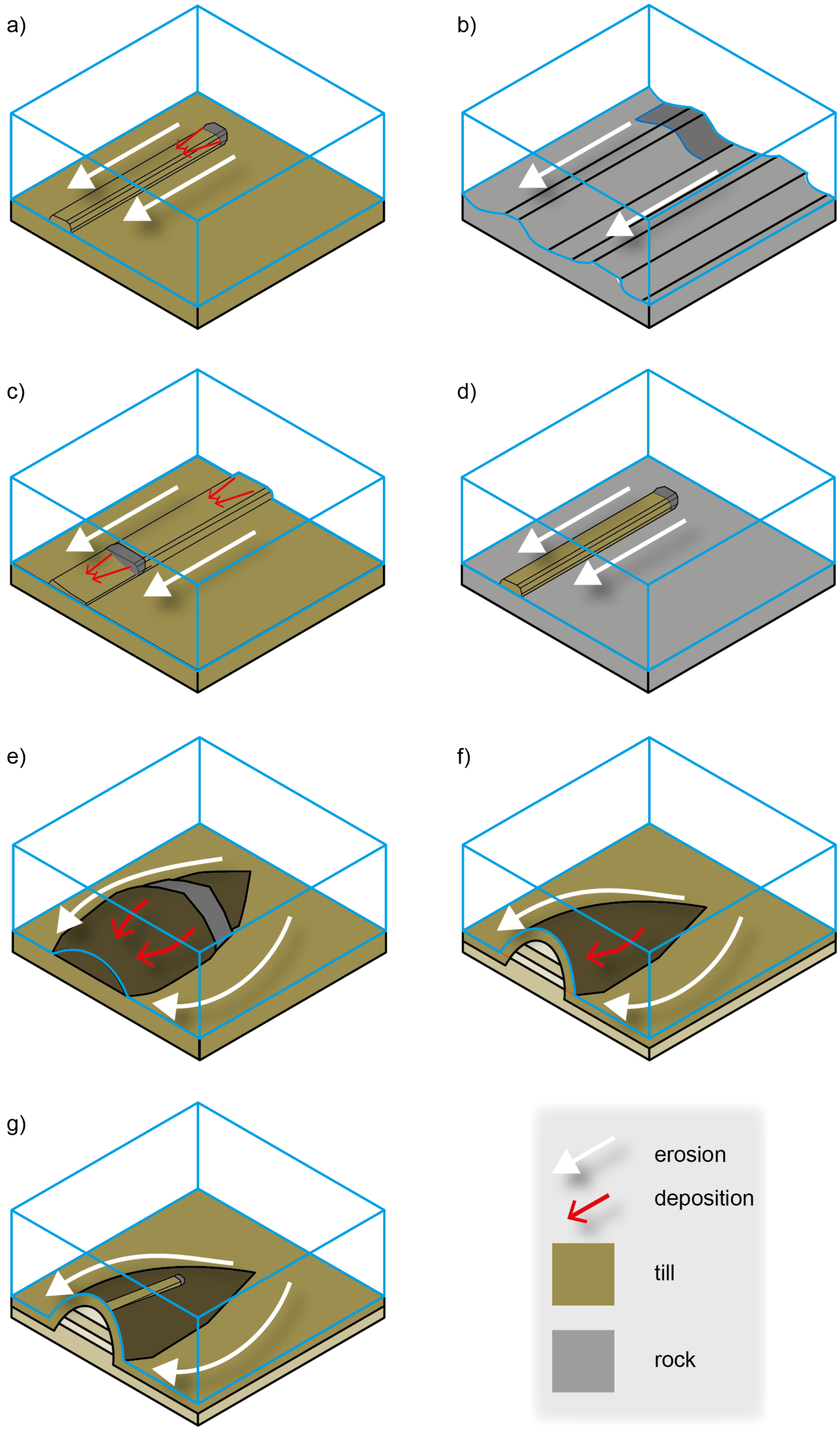

Figure 11. Schematic model for bedform formation (a) till flutes, (b) rock flutes, (c) composite flutes, (d) till flute on bedrock, (e) rock-cored drumlin, (f) erosional drumlin, (g) superimposition of smaller bedforms on larger bedforms.

Hart 2006a). Where there is a large stationary obstacle till may surround the core (Boyce & Eyles, 1991; Hart 1995a; Meehan et al. 1997; Chao Lu & Zhi Jiu, 2001; Fuller & Murray 2002) (rock-cored drumlin). Deposition will occur in the lee-side of the clast (in a similar way to the flute), with till erosion shaping the outside (Fig. 11e). Till fabrics within these drumlins are often oriented with the shape of the feature (Hill 1971; Hart, 1997). Where the obstacle is more rigid, then a drumlin will form from the erosion of the faster moving till (Fig. 11f), and produce the classic "erosional" drumlin where the internal form of the drumlin (which may be till or stratified sediments) bears no relationship with the drumlin form (Boyce & Eyles 1991; Hart 1997; Stokes et al. 2013a; Eyles et al. 2016). Till fabrics within the carapace will mirror the form of the drumlin (Hart 1997; Menzies & Brand 2007). Once any bedform is produced, smaller features such as flutes will be formed on top of it associated with the mobile clasts in the deforming layer passing over the larger bedform (Fig. 11g).

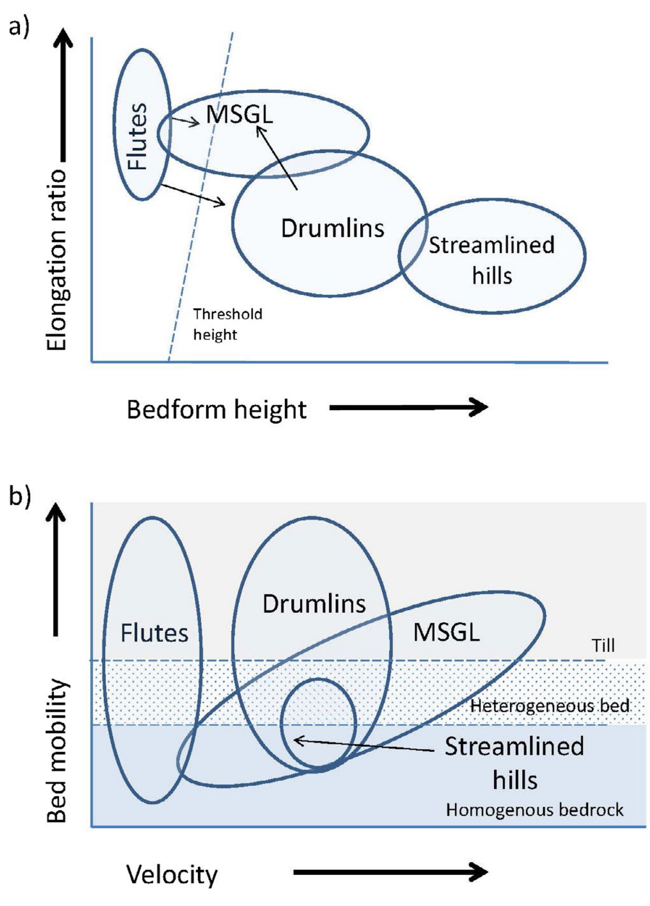

Figure 12. Bedform continuum: (a) schematic relationship between bedform height and elongation ratio; (b) schematic relationship between ice velocity and bed mobility.

In this way, both erosion and deposition are occurring at the same time. During flute formation, erosion occurred in the interflute areas, and deposition in the low pressure area behind the clasts. In the drumlin, the erosion is in the faster moving till in the interdrumlin areas, and deposition only if a low pressure area exists. The till in the carapace reflects the final deposition of the deforming bed itself.

Bedform continuum

Rose (1987) argued for a conceptual bedform continuum and presented a relationship between bedform length, elongation ratio, ice velocity and ice thickness (although Ely et al. 2016 have demonstrated there is both clustering and continuity between bedform shapes). The bedform continuum concept suggests that the bedforms of different scales are formed by similar processes. We present some variations on this classic schematic diagram. We suggest that the height of the bedform is a more important distinguishing factor than length, since the latter is already incorporated in the elongation ratio, and we have demonstrated the importance of a threshold height. Table 6 presents the mean height, elongation ratio and ice velocity from the different bedforms, and this is shown schematically in Fig. 12a.

At Skálafellsjökull we had evidence for flutes, large flutes and drumlins within the foreland. By definition MSGL's are large features, and extensive studies of their morphology, such as from Ely et al. (2016) are taken from Quaternary ice sheet sites (from satellite images) and the smallest 10th percentile are approximately 400 m long and 80 m wide. Bedforms of such large scale would be unlikely to form beneath valley glaciers and we suggest that the large flutes represented at Skálafellsjökull are a valley glacier/smaller scale equivalent to MSGL. Given the bedform continuum model, we argue that MSGL's are similarly formed by the same processes as flutes and drumlins (Hart 1997; Hindmarsh 1998b; King et al. 2009; Smith and Murray, 2009; Clarke 2010; Menzies et al. 2016, Stokes 2017).

We propose these different scale bedforms are related to bed mobility and velocity (Fig. 12b). We show the bed mobility as three general types: high mobility (till), intermediate mobility (heterogeneous bed, comprising mixed till and bedrock, jointed bedrock, deformable bedrock) and low mobility (homogeneous bedrock).

We suggest there are two possible pathways through the continuum. At low velocities flutes and drumlins form, but the difference between them is due to the threshold height of obstacles. It has been argued that as velocities increase drumlins will become elongated (Hollingworth 1931; Hart 1999; Stokes & Clark 2002; Stokes et al., 2013a). Sometimes drumlins become elongated into MSGL, so making distinguishing between the two landforms

Table 6. Typical sizes of streamlined bedforms.

	Mean height (m)	Mean elongation ratio	Mean velocity m a^{-1}
Flute (this study)	<0.2	~100	~10–30
Large flutes (this study)	<1	~10	~10–30
MSGL (King et al. 2007; Spagnolo et al. 2014; Ely et al. 2016)	1–9	2–200	>200
Drumlin (this study, Hart 1999; King et al. 2007; Spagnolo et al. 2012)	0.5–40	2–80	25–100
Streamlined hill (Rose 1987)	>50	<4	–

difficult (Graham et al. 2009; Stokes et al. 2013b, Spagnolo et al. 2014; Stokes 2017).

However, where flutes and MSGL are formed of bedrock or composite till and bedrock, they may be stationary in the landscape and may show no relationship between elongation and velocity. At Skálafellsjökull both large flutes and drumlins were probably formed under the same velocity regime, but related to different bedrock configurations. Under these conditions, increased velocity may lead to increased erosion, and increased relief of the bedforms, which has been reported from the literature (Spagnolo et al. 2014). In this way flutes may develop directly into MSGL's rather than passing through a drumlin phase.

Other researchers have noted the link between bedforms and bedrock type (Stokes & Clark 1999; Ó Cofaigh et al. 2002). Larter et al. (2014) and Graham et al. (2016) demonstrated how drumlins formed over hard crystalline bedrock with actively mobile sediment patches, whilst MSGL were formed on till overlying sedimentary rocks.

Thus the small scale features at Skalafellsjökull represent a good analogue for larger features formed beneath ice sheets, illustrating both the simultaneous erosion and deposition, the difference between flutes, large flutes (very small MSGLs), drumlins and but also demonstrating the importance of glacial history. We showed that beneath the glacier, till is deforming throughout the year, but at different rates. Where the bed has is heterogeneous, there will always be both mobile and stationary elements. Once deposition and erosion occur associated with these obstacles, these processes may continue in that location even after the obstacle has been removed. Thus subglacial beds may have a legacy element as they evolve over time.

Conclusion

This research (and the other related studies in Table 5) extends the previous large scale study by Hart (1997) into the examination of smaller bedforms. From these it is proposed that simultaneous deposition and erosion produces the full range of bedforms from flutes to drumlins. However, it is stressed that all these form due to a negative sediment flux (i.e., more sediment is removed from a given subglacial area than enters). Where there is a positive flux (i.e., more sediment enters a given subglacial area than is removed) there will be a net build up (deposition) of till.

There appears to be a growing consensus within the main drumlin theories. Within the instability theory (Hindmarsh 1998a; Fowler 2000; Stokes et al., 2013a) although this model is essentially a depositional one (building till hills from an initial surface and cannot account for flute formation in a mixed till/bedrock environment), Stoke et al. (2013a) discusses how the negative sediment flux element of the theory produces the erosional form of drumlins described in the literature. Similarly, the recent erodent layer hypothesis idea of Eyles et al. (2016) stresses the importance of erosion in drumlin formation. Whilst Iverson et al. (2017) and Möller and Dowling (2016) emphases the combined processes of deposition and erosion in drumlin formation.

We show that the subglacial environment at Skálafellsjökull comprised both erosional and depositional elements forming simultaneously. Due to the extensive fluting exposed in the foreland, we suggested that our *in situ* results may relate to flute forming processes. We showed that deformation within the till took place throughout the year, and that there were variations in till deformation over a relatively small area, and glacier speed-up events may have an effect on flute development. We were also able to make an estimation of the ice velocities associated with these processes (9.2–31 m a^{-1}) and show an erosion (by till or ice) rate on the bedrock flutes of 2.13 mm a^{-1}.

We demonstrated the formation of flutes associated with a mobile till bed. These form in the lee-side of core stones. However, where the obstacle was stationary or larger than a threshold height, then other forms of bedforms were produced. At Skálafellsjökull, stationary cores greater than the threshold height of 1.56 m led to the formation of rock-cored drumlins, whilst those less than the threshold height formed long wide large flutes (of rock and till). The latter are probably a good example of (very small) MSGL that have not formed from the elongation of drumlins, but rather the simultaneous deposition and erosion associated with stationary obstacles in the bed.

We discuss the subglacial bedform continuum in relation to elongation ratio and height, as well as bedform mobility and ice velocity. These form under a net erosional sediment flux. The bed in a heterogeneous mobility bedrock zone will be irregular with both mobile and stationary obstacles. At any one time, bedforms will develop which will be the result of active obstacles but also previous obstacles that have now been eroded away.

Thus, we have used a range of techniques to measure glacial processes, combined with detailed surveying, to understand the formation of an array of subglacial bedforms exposed in the foreland. We suggest these were formed from simultaneous deposition and erosion (by till and ice), under a net erosional regime, and reflect a subglacial bedform continuum based on bedform height, elongation ratio, bed mobility and ice velocity.

Acknowledgements

The authors would like to thank the Glacsweb team 2008–2013 for field support and specifically Dr Andrew Turner and Dr Tom Bishop for UAV field support. We would also like to thank Mark Dover from the Cartographic Unit for figure drawing. We would also like to thank Ívar Örn Benediktsson and an anonymous reviewer for their helpful comments in improving the manuscript.

Disclosure statement

No potential conflict of interest was reported by the authors.

Funding

This research was funded by EPSRC [grant number EP/C511050/1], Leverhulme [grant number F/00 180/AK], National Geographic [grant number GEFNE45-12] and NERC [studentship AIC]. The GPR and Leica 1200 GPS units were loaned from the NERC Geophysical Equipment Facility.

References

Alley, R.B., Blankenship, D.D., Bentley, C.R. & Rooney, S.T., 1986: Deformation of till beneath ice stream B, West Antarctica. *Nature 322*, 57–59.

Anderson, R.S., Anderson, S.P., MacGregor, K.R., Waddington, E.D., O'Neel, S., Riihimaki, C.A. & Loso, M.G., 2004: Strong feedbacks between hydrology and sliding of a small alpine glacier. *Journal of Geophysical Research: Earth Surface 109*, 2156–2202.

Barchyn, T.E., Dowling, T.P., Stokes, C.R. & Hugenholtz, C.H., 2016: Subglacial bed form morphology controlled by ice speed and sediment thickness. *Geophysical Research Letters 43*(14), 7572–7580.
Benn, D.I., 1994: Fluted moraine formation and till genesis below a temperate valley glacier: Slettmarkbreen, Jotunheimen, southern Norway. *Sedimentology 41*, 279–292.
Benediktsson, Í.Ö., Jónsson, S.A., Schomacker, A., Johnson, M.D., Ingólfsson, Ó., Zoet, L., Iverson, N.R. & Stötter, J., 2016: Progressive formation of modern drumlins at Múlajökull, Iceland: stratigraphical and morphological evidence. *Boreas 45*(4), 567–583.
Blake, E., Clarke, G.K. & Gérin, M.C., 1992: Tools for examining subglacial bed deformation. *Journal of Glaciology 38*(130), 388–396.
Boulton, G.S., 1976: The origin of glacially fluted surfaces: observations and theory. *Journal of Glaciology 17*, 287–309.
Boulton, G.S., 1982: Processes and patterns of glacial erosion. *In*: *Glacial geomorphology*, 41–87. Springer, Dordrecht.
Boulton, G.S., 1987: A theory of drumlin formation by subglacial deformation. *In* J. Menzies & J. Rose (eds.): *Drumlin Symposium*, 25–80. Balkema, Rotterdam.
Boulton, G.S., Dobbie, K.E. & Zatsepin, S., 2001: Sediment deformation beneath glaciers and its coupling to the subglacial hydraulic system. *Quaternary International 86*(1), 3–28.
Boulton, G.S. & Jones, A.S., 1979: Stability of temperate ice caps and ice sheets resting on beds of deformable sediment. *Journal of Glaciology 24*, 29–44.
Boyce, J.I. & Eyles, N., 1991: Drumlins carved by deforming till streams below the Laurentide ice sheet. *Geology 19*, 787–790.
Braithwaite, R.J., 1995: Positive degree-day factors for ablation on the Greenland ice sheet studied by energy-balance modelling. *Journal of Glaciology 41*(137), 153–160.
Brown, N.E., Hallet, B. & Booth, D.B., 1987: Rapid soft bed sliding of the Puget glacial lobe. *Journal of Geophysical Research: Solid Earth 92*(B9), 8985–8997.
Chandler, B.M., Evans, D.J. & Roberts, D.H., 2016a: Characteristics of recessional moraines at a temperate glacier in SE Iceland: insights into patterns, rates and drivers of glacier retreat. *Quaternary Science Reviews 135*, 171–205.
Chandler, B.M., Evans, D.J., Roberts, D.H., Ewertowski, M. & Clayton, A.I., 2016b: Glacial geomorphology of the Skálafellsjökull foreland, Iceland: a case study of 'annual'moraines. *Journal of Maps 12*(5), 904–916.
Chao Lu, Y. & Zhi Jiu, C., 2001: Subglacial deformation: evidence from microfabric studies of particles and voids in till from the upper Ürümqi river valley, Tien Shan, China. *Journal of Glaciology 47*(159), 607–612.
Clark, C.D., 2010: Emergent drumlins and their clones: from till dilatancy to flow instabilities. *Journal of Glaciology 56*(200), 1011–1025.
Clark, C.D., Hughes, A.L., Greenwood, S.L., Spagnolo, M. & Ng, F.S., 2009: Size and shape characteristics of drumlins, derived from a large sample, and associated scaling laws. *Quaternary Science Reviews 28*(7), 677–692.
Clarke, G.K.C., 1987: Subglacial till: a physical framework for its properties and processes. *Journal of Geophysical Research 92*(B9), 8942–8984.
Crosby, I.B., 1934: Evidence from drumlins concerning the glacial history of Boston Basin. *Geological Society of America, Bulletin 45*, 135–158.
Cuffey, K. & Alley, R.B., 1996: Is erosion by deforming subglacial sediments significant? (Toward till continuity). *Annals of Glaciology 22*(1), 17–24.
Dowling, T.P., Möller, P. & Spagnolo, M., 2016: Rapid subglacial streamlined bedform formation at a calving bay margin. *Journal of Quaternary Science 31*(8), 879–892.
Dowling, T.P., Spagnolo, M. & Möller, P., 2015: Morphometry and core type of streamlined bedforms in southern Sweden from high resolution LiDAR. *Geomorphology 236*, 54–63.
Dyson, J.L., 1952: Ice-ridged moraines and their relation to glaciers [Montana]. *American Journal of Science 250*(3), 204–211.
Ely, J.C., Clark, C.D., Spagnolo, M., Stokes, C.R., Greenwood, S.L., Hughes, A.L., Dunlop, P. & Hess, D., 2016: Do subglacial bedforms comprise a size and shape continuum? *Geomorphology 257*, 108–119.
Ely, J.C., Graham, C., Barr, I.D., Rea, B.R., Spagnolo, M. & Evans, J., 2017: Using UAV acquired photography and structure from motion techniques for studying glacier landforms: application to the glacial flutes at Isfallsglaciären. *Earth Surface Processes and Landforms 42*(6), 877–888.
Eyles, N., Boyce, J. & Putkinen, N., 2015: Neoglacial (< 3000 years) till and flutes at Saskatchewan Glacier, Canadian Rocky Mountains, formed by subglacial deformation of a soft bed. *Sedimentology 62*(1), 182–203.
Eyles, N., Putkinen, N., Sookhan, S. & Arbelaez-Moreno, L., 2016: Erosional origin of drumlins and megaridges. *Sedimentary Geology 338*, 2–23.
Fowler, A.C., 2000: An instability mechanism for drumlin formation. *Geological Society, London, Special Publications 176*(1), 307–319.
Fowler, A.C., 2009: Instability modelling of drumlin formation incorporating lee-side cavity growth. *Proceedings of the Royal Society of London A: Mathematical, Physical and Engineering Sciences 465* (2109), 2681–2702.
Fowler, A.C., Spagnolo, M., Clark, C.D., Stokes, C.R., Hughes, A.L.C. & Dunlop, P., 2013: On the size and shape of drumlins. *GEM-International Journal on Geomathematics 4*(2), 155–165.
Frey, H. & Paul, F., 2012: On the suitability of the SRTM DEM and ASTER GDEM for the compilation of topographic parameters in glacier inventories. *International Journal of Applied Earth Observation and Geoinformation 18*, 480–490.
Fuller, S. & Murray, T., 2002: Sedimentological investigations in the forefield of an Icelandic surge-type glacier: implications for the surge mechanism. *Quaternary Science Reviews 21*, 1503–1520.
Gjessing, J., 1965: On 'plastic scouring'and 'subglacial erosion'. *Norsk Geografisk Tidsskrift 20*, 1–37.
Graham, A.G., Larter, R.D., Gohl, K., Hillenbrand, C.D., Smith, J.A. & Kuhn, G., 2009: Bedform signature of a West Antarctic palaeo-ice stream reveals a multi-temporal record of flow and substrate control. *Quaternary Science Reviews 28*(25), 2774–2793.
Graham, A.G., Nitsche, F.O., Larter, R.D. & Gohl, K., 2016: Submarine landform assemblage produced beneath the Dotson-Getz palaeo-ice stream, West Antarctica. *Geological Society, London, Memoirs 46*(1), 345–348.
Greenwood, S.L. & Clark, C.D., 2008: Subglacial bedforms of the Irish ice sheet. *Journal of Maps 4*(1), 332–357.
Guðnason, B., 1957: *Sýslulýsingar 1744–1749 [County Descriptions 1744–1749]*. Sögufélagið, Reykjavík. [In Icelandic].
Hackney, C. & Clayton, A., 2015: Section 2.1.7. Unmanned Aerial Vehicles (UAVs) and their application in geomorphic mapping. *In*: S.J. Cook, L.E. Clarke & J.M. Nield (eds.): *Geomorphological techniques* (Online Edition). British Society for Geomorphology, London. ISSN: 2047-0371.
Hallet, B., Hunter, L. & Bogen, J., 1996: Rates of erosion and sediment evacuation by glaciers: a review of field data and their implications. *Global and Planetary Change 12*, 213–235.
Hannesdóttir, H., Björnsson, H., Pálsson, F., Aðalgeirsdóttir, G. & Guðmundsson, S., 2015: Variations of southeast Vatnajökull ice cap (Iceland) 1650–1900 and reconstruction of the glacier surface geometry at the Little Ice Age maximum. *Geografiska Annaler: Series A, Physical Geography 97*, 237–264.
Hart, J.K., 1995a: Drumlins, flutes and lineations at Vestari-Hagafellsjökull, Iceland. *Journal of Glaciology 41*, 596–606.
Hart, J.K., 1995b: An investigation of the deforming layer/debris-rich basal-ice continuum, illustrated from three Alaskan glaciers. *Journal of Glaciology 41*(139), 619–633.
Hart, J.K., 1997: The relationship between drumlins and other forms of subglacial glaciotectonic deformation. *Quaternary Science Reviews 16*(1), 93–107.
Hart, J.K., 1999: Identifying fast ice flow from landform assemblages in the geological record: a discussion. *Annals of Glaciology 28*(1), 59–66.
Hart, J.K., 2006a: Athabasca Glacier, Canada–a field example of subglacial ice and till erosion? *Earth Surface Processes and Landforms 31*(1), 65–80.
Hart, J.K., 2006b: An investigation of subglacial processes at the microscale from Briksdalsbreen, Norway. *Sedimentology 53*(1), 125–146.
Hart, J.K., 2017: Subglacial till formation: microscale processes within the subglacial shear zone. *Quaternary Science Reviews 170*, 26–44.
Hart, J.K. & Boulton, G.S., 1991: The interrelationship between glaciotectonic deformation and glaciodeposition within the glacial environment. *Quaternary Science Reviews 10*, 335–350.
Hart, J.K., Hindmarsh, R.C.A. & Boulton, G.S., 1990: Different styles of subglacial glaciotectonic deformation in the context of the Anglian ice sheet. *Earth Surface Processes and Landforms 15*, 227–241.

Hart, J.K. & Martinez, K., 2006: Environmental sensor networks: a revolution in the earth system science? *Earth-Science Reviews 78*(3), 177–191.
Hart, J.K., Martinez, K., Ong, R., Riddoch, A., Rose, K.C. & Padhy, P., 2006: A wireless multi-sensor subglacial probe: design and preliminary results. *Journal of Glaciology 52*(178), 389–397.
Hart, J.K., Rose, K.C., Clayton, A. & Martinez, K., 2015: Englacial and subglacial water flow at Skálafellsjökull, Iceland derived from ground penetrating radar, *in situ* Glacsweb probe and borehole water level measurements. *Earth Surface Processes and Landforms 40*(15), 2071–2083.
Hart, J.K., Rose, K.C., Martinez, K. & Ong, R., 2009: Subglacial clast behaviour and its implication for till fabric development: new results derived from wireless subglacial probe experiments. *Quaternary Science Reviews 28*(7–8), 597–607.
Hart, J.K. & Smith, B., 1997: Subglacial deformation associated with fast ice flow, from the Columbia Glacier. *Alaska. Sedimentary Geology 111*(1–4), 177–197.
Hiemstra, J.F. & Rijsdijk, K.F., 2003: Observing artificially induced strain: implications for subglacial deformation. *Journal of Quaternary Science 18*, 373–383.
Hicock, S.R. & Dreimanis, A., 1992: Deformation till in the Great Lakes region: implications for rapid flow along the south-central margin of the Laurentide Ice Sheet. *Canadian Journal of Earth Sciences 29*, 1565–1579.
Hill, A.R., 1971: The internal composition and structure of drumlins in North Down and South Antrim, Northern Ireland. *Geografiska Annaler: Series A, Physical Geography 53*(1), 14–31.
Hillier, J.K., Smith, M.J., Clark, C.D., Stokes, C.R. & Spagnolo, M., 2013: Subglacial bedforms reveal an exponential size–frequency distribution. *Geomorphology 190*, 82–91.
Hillier, J.K. (this special issue).
Hindmarsh, R.C., 1998a: The stability of a viscous till sheet coupled with ice flow, considered at wavelengths less than the ice thickness. *Journal of Glaciology 44*(147), 285–292.
Hindmarsh, R.C., 1998b: Drumlinization and drumlin-forming instabilities: viscous till mechanisms. *Journal of Glaciology 44*(147), 293–314.
Hindmarsh, R.C., 1999: Coupled ice–till dynamics and the seeding of drumlins and bedrock forms. *Annals of Glaciology 28*(1), 221–230.
Hock, R., 2003: Temperature index melt modelling in mountain areas. *Journal of Hydrology 282*(1), 104–115.
Hollingworth, S.E., 1931: Glaciation of western Edenside and adjoining areas and the drumlins of the Edenside and Solway basin. *Quarterly Journal of the Geological Society of London 87*, 281–359.
Hooyer, T.S. & Iverson, N.R., 2000: Clast-fabric development in a shearing granular material: implications for subglacial till and fault gouge. *Geological Society of America Bulletin 112*(5), 683–692.
Hoppe, G. & Schytt, V., 1953: Some observations on fluted moraine surfaces. *Geografiska Annaler 35*(2), 105–115.
Hubbard, B. & Nienow, P., 1997: Alpine subglacial hydrology. *Quaternary Science Reviews 16*(9), 939–955.
Hughes, A.L., Clark, C.D. & Jordan, C.J., 2010: Subglacial bedforms of the last British Ice Sheet. *Journal of Maps 6*(1), 543–563.
Iken, A., Röthlisberger, H., Flotron, A. & Haeberli, W., 1983: The uplift of Unteraargletscher at the beginning of the melt season—a consequence of water storage at the bed? *Journal of Glaciology 29*(101), 28–47.
Iverson, N.R., 2010: Shear resistance and continuity of subglacial till: hydrology rules. *Journal of Glaciology 56*(200), 1104–1114.
Iverson, N.R., McCracken, R.G., Zoet, L.K., Benediktsson, Í.Ö., Schomacker, A., Johnson, M.D. & Woodard, J., 2017: A theoretical model of drumlin formation based on observations at Múlajökull, Iceland. *Journal of Geophysical Research: Earth Surface 122*(12), 2302–2323.
Johannesson, T., Sigurdsson, O., Laumann, T. & Kennett, M., 1995: Degree-day glacier mass-balance modelling with applications to glaciers in Iceland, Norway and Greenland. *Journal of Glaciology 41*(138), 345–358.
Johnson, M.D., Schomacker, A., Benediktsson, Í.Ö., Geiger, A.J., Ferguson, A. & Ingólfsson, Ó., 2010: Active drumlin field revealed at the margin of Múlajökull, Iceland: a surge-type glacier. *Geology 38*(10), 943–946.
Jónsson, S.A., Benediktsson, Í.Ö., Ingólfsson, Ó., Schomacker, A., Bergsdóttir, H.L., Jacobson, W.R. & Linderson, H. 2016: Submarginal drumlin formation and late Holocene history of Fláajökull, southeast Iceland. *Annals of Glaciology* 57, 128–141.
Jónsson, S.A., Schomacker, A., Benediktsson, Í.Ö., Ingólfsson, Ó. & Johnson, M.D., 2014: The drumlin field and the geomorphology of the Múlajökull surge-type glacier, central Iceland. *Geomorphology 207*, 213–220.
Karlén, W., 1981: Flutes on bare bedrock. *Journal of Glaciology 27*(95), 190–192.
King, E.C., Woodward, J. & Smith, A.M., 2007: Seismic and radar observations of subglacial bed forms beneath the onset zone of Rutford Ice Stream. *Antarctica. Journal of Glaciology 53*(183), 665–672.
King, E.C., Hindmarsh, R.C. & Stokes, C.R., 2009: Formation of mega-scale glacial lineations observed beneath a West Antarctic ice stream. *Nature Geoscience 2*(8), 585–588.
Larter, R.D., Anderson, J.B., Graham, A.G., Gohl, K., Hillenbrand, C.D., Jakobsson, M., Johnson, J.S., Kuhn, G., Nitsche, F.O., Smith, J.A. & Witus, A.E., 2014: Reconstruction of changes in the Amundsen Sea and Bellingshausen sea sector of the West Antarctic ice sheet since the last glacial maximum. *Quaternary Science Reviews 100*, 55–86.
Lawler, D.M., Dolan, M., Tomasson, H. & Zophoniasson, S., 1992: Temporal variability of suspended sediment flux from a subarctic glacial river, southern Iceland. In: Erosion and Sediment Transport Monitoring Programs in River Basins. Proc. Oslo Symp. IAHS Publ *210*, 233–243.
Martinez, K., Hart, J.K., Basford, P.J., Bragg, G.M., Ward, T. & Young, D.S., 2017: A geophone wireless sensor network for investigating glacier stick-slip motion. *Computers & Geosciences 105*, 103–112.
Martinez, K., Hart, J.K. & Ong, R., 2004: Environmental sensor networks. *Computer 37*, 50–56.
Martinez, K., Hart, J.K. & Ong, R., 2009: Deploying a wireless sensor network in Iceland. In *International conference on GeoSensor Networks*, 131–137. Springer, Berlin, Heidelberg.
McCracken, R.G., Iverson, N.R., Benediktsson, Í.Ö., Schomacker, A., Zoet, L.K., Johnson, M.D., Hooyer, T.S. & Ingólfsson, Ó., 2016: Origin of the active drumlin field at Múlajökull, Iceland: new insights from till shear and consolidation patterns. *Quaternary Science Reviews 148*, 243–260.
Meehan, R.T., Warren, W.P. & Gallagher, C.J., 1997: The sedimentology of a Late Pleistocene drumlin near Kingscourt. *Ireland. Sedimentary Geology 111*(1–4), 91–105.
van der Meer, J.J., 1993: Microscopic evidence of subglacial deformation. *Quaternary Science Reviews 12*(7), 553–587.
Menzies, J., 1979: Mechanics of drumlin formation. *Journal of Glaciology 27*, 372–384.
Menzies, J. & Brand, U., 2007: The internal sediment architecture of a drumlin, Port Byron, New York State, USA. *Quaternary Science Reviews 26*(3–4), 322–335.
Menzies, J., Hess, D.P., Rice, J.M., Wagner, K.G. & Ravier, E., 2016: A case study in the New York Drumlin Field, an investigation using microsedimentology, resulting in the refinement of a theory of drumlin formation. *Sedimentary Geology 338*, 84–96.
Moberg, A., Sonechkin, D.M., Holmgren, K., Datsenko, N.M. & Karlén, W., 2005: Highly variable Northern Hemisphere temperatures reconstructed from low- and high-resolution proxy data. *Nature 433*, 613–617.
Möller, P. & Dowling, T.P., 2016: Streamlined subglacial bedforms on the Närke plain, south-central Sweden–areal distribution, morphometrics, internal architecture and formation. *Quaternary Science Reviews 146*, 182–215.
Murray, T. & Clarke, G.K., 1995: Black-box modeling of the subglacial water system. *Journal of Geophysical Research: Solid Earth 100*(B6), 10231–10245.
Ó Cofaigh, C., Pudsey, C.J., Dowdeswell, J.A. & Morris, P., 2002: Evolution of subglacial bedforms along a paleo-ice stream, Antarctic Peninsula continental shelf. *Geophysical Research Letters 29*(8), 41-1–41-4.
Ólafsson, E. & Pálsson, B., 1981: *Ferðabók Eggerts Ólafssonar og Bjarna Pálssonar: um ferðir þeirra á Íslandi árin 1752–1757* [The Travel Book of Eggert Ólafsson and Bjarni Pálsson: about their Travels in Iceland in 1752–1757], 2nd ed. Örn og Örlygur, Reykjavík. [In Icelandic].

Patterson, C.J. & Hooke, R.L., 1995: Physical environment of drumlin formation. *Journal of Glaciology 41*(137), 30–38.

Pritchard, H., Murray, T., Luckman, A., Strozzi, T. & Barr, S., 2005: Glacier surge dynamics of Sortebræ, east Greenland, from synthetic aperture radar feature tracking. *Journal of Geophysical Research 110*, F03005. doi: https://doi.org/10.1029/2004JF000233.

Rees, W.G., 2012: Assessment of ASTER global digital elevation model data for Arctic research. *Polar Record 48*(1), 31–39.

Roberson, S.A.M., Hubbard, B., Coulson, H.R. & Boomer, I., 2011: Physical properties and formation of flutes at a polythermal valley glacier: Midre Lovénbreen, Svalbard. *Geografiska Annaler: Series A, Physical Geography 93*(2), 71–88.

Rose, J., 1987: Drumlins as part of a glacier bedform continuum. *In* J. Menzies & J. Rose (eds.): *Drumlin Symposium*, 103–116. Balkema, Rotterdam.

Rose, J., 1989: Glacier stress patterns and sediment transfer associated with the formation of superimposed flutes. *Sedimentary Geology 62*(2–4), 151–176.

Schomacker, A., Benediktsson, Í.Ö. & Ingólfsson, Ó., 2014: The Eyjabakkajökull glacial landsystem, Iceland: geomorphic impact of multiple surges. *Geomorphology 218*, 98–107.

Schomacker, A., Benediktsson, Í.Ö., Ingólfsson, Ó., Friis, B., Korsgaard, N.J., Kjær, K.H. & Keiding, J.K., 2012: Late Holocene and modern glacier changes in the marginal zone of Sólheimajökull, South Iceland. *Jökull 62*, 111–130.

Schoof, C., 2002: *Mathematical models of glacier sliding and drumlin formation*. Doctoral dissertation. University of Oxford.

Schoof, C., 2007: Pressure-dependent viscosity and interfacial instability in coupled ice–sediment flow. *Journal of Fluid Mechanics 570*, 227–252.

Schoof, C.G. & Clarke, G.K., 2008: A model for spiral flows in basal ice and the formation of subglacial flutes based on a Reiner-Rivlin rheology for glacial ice. *Journal of Geophysical Research: Solid Earth 113*(B5), B05204.

Shaw, J. & Freschauf, R.C., 1973: A kinematic discussion of the formation of glacial flutings. *The Canadian Geographer/Le Géographe Canadien 17*(1), 19–35.

Sigurðsson, O., 1998: Glacier variations in Iceland 1930-1995. *Jökull 45*, 3–25.

Smith, A.M., Bentley, C.R., Bingham, R.G. & Jordan, T.A., 2012: Rapid subglacial erosion beneath Pine Island glacier, west Antarctica. *Geophysical Research Letters 39*, 1–5.

Smith, A.M. & Murray, T., 2009: Bedform topography and basal conditions beneath a fast-flowing West Antarctic ice stream. *Quaternary Science Reviews 28*(7), 584–596.

Smith, A., Murray, T., Nicholls, K., Makinson, K., Aðalgeirsdóttir, G., Behar, A. & Vaughan, D., 2007: Rapid erosion, drumlin formation, and changing hydrology beneath an Antarctic ice stream. *Geology 35*, 127–130.

Snavely, N., Seitz, S.M. & Szeliski, R., 2008: Modeling the world from internet photo collections. *International Journal of Computer Vision 80*(2), 189–210.

Spagnolo, M., Clark, C.D., Ely, J.C., Stokes, C.R., Anderson, J.B., Andreassen, K., Graham, A.G. & King, E.C., 2014: Size, shape and spatial arrangement of mega-scale glacial lineations from a large and diverse dataset. *Earth Surface Processes and Landforms 39*(11), 1432–1448.

Spagnolo, M., Clark, C.D. & Hughes, A.L., 2012: Drumlin relief. *Geomorphology 153*, 179–191.

Stokes, C.R., 2017: Geomorphology under ice streams: moving from form to process. *Earth Surface Processes and Landforms 43*, 85–123.

Stokes, C.R. & Clark, C.D., 1999: Geomorphological criteria for identifying Pleistocene ice streams. *Annals of Glaciology 28*, 67–74.

Stokes, C.R. & Clark, C.D., 2002: Ice stream shear margin moraines. *Earth Surface Processes and Landforms 27*(5), 547–558.

Stokes, C.R., Fowler, A.C., Clark, C.D., Hindmarsh, R.C.A. & Spagnolo, M., 2013a: The instability theory of drumlin formation and its explanation of their varied composition and internal structure. *Quaternary Science Reviews 62*, 77–96.

Stokes, C.R., Spagnolo, M. & Clark, C.D., 2011: The composition and internal structure of drumlins: complexity, commonality, and implications for a unifying theory of their formation. *Earth-Science Reviews 107*(3), 398–422.

Stokes, C.R., Spagnolo, M., Clark, C.D., Cofaigh, C.Ó., Lian, O.B. & Dunstone, R.B., 2013b: Formation of mega-scale glacial lineations on the Dubawnt Lake Ice Stream bed: 1. Size, shape and spacing from a large remote sensing dataset. *Quaternary Science Reviews 77*, 190–209.

Sugiyama, S., Bauder, A., Riesen, P. & Funk, M., 2010: Surface ice motion deviating toward the margins during speed-up events at Gornergletscher, Switzerland. *Journal of Geophysical Research: Earth Surface 115*(F3), F04019.

van der Wateren, F.M., Kluiving, S.J. & Bartek, L.R., 2000: Kinematic indicators of subglacial shearing. *Geological Society, London, Special Publications 176*, 259–278.

Westoby, M.J., Brasington, J., Glasser, N.F., Hambrey, M.J. & Reynolds, J.M., 2012: 'Structure-from-Motion' photogrammetry: a low-cost, effective tool for geoscience applications. *Geomorphology 179*, 300–314.

Willis, I.C., 1995: Intra-annual variations in glacier motion: a review. *Progress in Physical Geography 19*(1), 61–106.

Vinther, B.M., Buchardt, S.L., Clausen, H.B., Dahl-Jensen, D., Johnsen, S.J., Fisher, D.A., Koerner, R.M., Raynaud, D., Lipenkov, V., Andersen, K.K., Blunier, T., Rasmussen, S.O., Steffensen, J.P. & Svensson, A.M., 2009: Holocene thinning of the Greenland ice sheet. *Nature 461*, 385–388.

Þorkelsson, J., 1918–1920: *Jarðabók Ísleifs sýslumanns Einarssonar yfir Austur-Skaptafellssýslu í umboði Árna Magnússonar 1708–1709* [The book of farms in Austur-Skaftafellssýsla 1708–1709 by the county governor Ísleifur Einarsson by the commission of Árni Magnússon], *Blanda – Fróðleikur gamall og nýr* [Blanda – Old and New Knowledge]. Sögufélagið, Reykjavík. 1–38. [In Icelandic].